Chapter 9
System Capacity

Fernando J. Velez, M. Kashif Nazir, A. Hamid Aghvami, Oliver Holland, and Daniel Robalo

Abstract In Fixed WiMAX, the contribution from each transmission mode can be incorporated into an implicit formulation to obtain the supported throughput as a function of the carrier-to-interference ratio. This is done by weighting the physical throughput in each concentric coverage ring by the size of the ring. In this paper, multi-hop cells are formed by a central coverage zone and three outer coverage zones served by cheaper low-complexity relays. It is assumed that line of sight propagation to the bases station is achieved in a high percentage of the cell, reducing the impact of selective fading, through allowing dimensioning to be done by GIS cellular planning tools. By using tri-sectorised equipment there is a need for three times more bandwidth, while hardware costs are higher. In our proposal for relays, the FDD mode is considered and the frames need to guarantee resources for BS-to-MS communications but also for BS-to-RS and RS-to-MS communications. These requirements leads to a 1/5 asymmetry factor between the UL and DL in the omnidirectional BS case and to a 3/7 asymmetry factor in the case of tri-sectored BSs. Although the reuse distance is augmented by a factor $\sqrt{3}$, we show that with the use of relays in FDD mode only the consideration of tri-sectored BSs with reuse pattern $K = 3$ (at the cost of extra channels, corresponding to 9 channels) enables to obtain values for the throughput comparable to cases without the use of relays. The presence of sub-channelisation only improves the results for the highest values of R. The consideration of tri-sectored BS antennas with $K = 1$ (whilst keeping the number of required channels – equal to 3) did not enable to obtain values of the throughput comparable to the ones without using relays, although frame format is more favourable. Relays can be cheaper than BS with full functionalities. As the use of relays may lead to lower costs it is worthwhile to analyse the impact of using them on costs and revenues.

F.J. Velez (✉)
Instituto de Telecomunicações-DEM, Universidade da Beira Interior, Calçada Fonte do Lameiro, 6201-001, Covilhã, Portugal
e-mail: fjv@ubi.pt

R. Prasad and F.J. Velez, *WiMAX Networks*,
DOI 10.1007/978-90-481-8752-2_9,

9.1 Introduction

In the context of Worldwide Interoperability for Microwave Access (WiMAX) planning, research on the variation of the carrier-to-noise-plus-interference ratio (CNIR), against different system parameters, is of fundamental importance. As there are challenges in both the uplink (UL) and downlink (DL) in WiMAX, techniques such as sub-channelisation may be applied to reduce the impact of noise on link performance. However, only Mobile WiMAX allows for sub-channelisation in both the UL and DL; fixed WiMAX only allows for it in the UL this absence of sub-channelisation in the DL for fixed WiMAX may be a cause of performance degradation (mainly owing to the extra noise caused by the larger spectrum bandwidth). For cellular planning purposes, the UL and DL CNIRs from/at the wireless Subscriber Station (SS) are very significant parameters.

From a detailed analysis of CNIR variation for different coverage and reuse distances, an evaluation of the achievable reuse patterns can be performed for different modulation and coding schemes (MCSs). In order to more effectively use radio frequency spectrum, it is important to choose a frequency reuse scheme that leads to coverage guarantee and improved system capacity whilst minimising interference.

Broadband wireless access enabling the operation of multi-hop relay stations (RSs) aims not only to enhance the coverage but also the system capacity, as interference is mitigated owing to the lowest transmitter power associated to the small range of the RSs. Compared with base stations (BSs), RSs does not need a wire-line backhaul and has much lower hardware complexity; hence, using RSs can significantly reduce the deployment cost of the system. The main objective is to achieve the highest values for the carrier-to-interference ratio, C/I, and, in return, the maximum supported throughput, by using relays for a given frequency reuse pattern, for example, $K = 3$.

In this work, a comparison of the different values the throughput is performed between the RSs, BSs and SSs in topologies with relays. By weighting the physical throughput in each concentric cell coverage ring by the size of the ring, the contribution from each transmission mode (or MCS) is included in an implicit function formulation to obtain the average supported throughput. For consecutive MCSs, the step distances are determined by the correspondence between minimum values at the CNIR curves (for a given MCS) and the supported physical throughput by an inversion procedure (via the consideration of each MCS stepwise threshold).

The remaining of this Chapter is organized as follows. Sections 9.2 and 9.3 presents the formulations and assumptions for the CNIR analysis in the DL and UL, for configurations without and with relays for fixed WiMAX configurations. The supported physical throughput is analyzed in Section 9.4, envisaging the cases without relays and with relays (DL and UL) Section 9.5 addresses the special case of unitary reuse pattern, where the use relays may present a slight advantage. Finally, Section 9.6 presents the conclusions.

9.2 *CNIR* Versus Physical Throughput Without Relays

In Fixed WiMAX, the supported physical user throughput is a function of the supported MCS, which in turn depends on the achievable *CNIR* compared with the minimum *CNIR*, $CNIR_{min}$, for each MCS (see Tables 8.2 and 8.16). It is therefore important to analyse the evolution of the *CNIR* against choices of several system parameters as well as the chosen co-channel reuse factor.

If Frequency Division Duplexing (FDD) is used, analytical modelling of coverage and frequency reuse problems can only be carried out in Fixed WiMAX. Our chosen approach simultaneously accounts for carrier-to-noise and carrier-to-interference constraints [1, 2].

Figure 9.1 presents the distance associated with coverage and interference for a 2D geometry with six interferers, when the mobile user is at a distance d from its serving base station (BS). The worst-case scenario in the DL occurs when the BS of the serving cell transmits to the most distant possible location of subscriber station (SS) it is serving, using a channel (or sub-channel) on which the SS is also receiving interference from the BSs of the six co-channel hexagonal neighbouring co-cells. If d is replaced by R the cell coverage distance or radius ($0 \leq d \leq R$), this worst case is as depicted in Fig. 9.1. Note that if D is the reuse distance, there are tiers of interference at distances D, $2D$, etc. However, if a high value for the propagation decay exponent is set, it is a valid approximation to only consider the first tier of interference, as shown in Fig. 9.1.

In the UL, the worst-case scenario occurs when the SS is transmitting to the BS from the cell edge, while interfering mobiles are on the boundary between interfering cells' edges and the serving cell of the SS [3]. When sectorization is considered, the number of interfering cells is decreased and system capacity increases. Such coverage and reuse geometries are commonly found in rural and suburban environments. In urban areas, owing to the obstruction of buildings and other urban obstacles, perfect circular/hexagonal cell coverage cannot be assumed anymore.

Here we assume the use of the modified Friis propagation model [3], and that values of the transmitter power, propagation exponent, and transmitter and receiver antenna gains are set at $P_t = -2$ dBW, $\gamma = 3$, $G_t = 17$ dBi, and $G_r = 9$ dBi, respectively. The radio frequency bandwidth, noise figure, and frequency are $b_{rf} = 3.5$ MHz, $N_f = 3$ dB, and $f = 3.5$ GHz. The values of these parameters are extracted from the experimental fixed WiMAX demonstrator from [4].

In contrast with Mobile WiMAX, a limitation of IEEE 802.16-2004 is that it does not support sub-channelisation on the DL [5]. On the UL, the use of sub-channelisation allows SS transmissions to only use 1/16 of the bandwidth assigned to transmissions from the BS, leading to a 12 dB link budget improvement [6]. The IEEE 802.16-2004 standard defines 16 sub-channels, where either 1, 2, 4, 8 or all sub-channels can be assigned to a SS. Each user in each different sub-channel may use a different MCS in successive bursts as long as he/she is using a different sub-channel. Nevertheless, it is a worth noting that in the DL, because the MCS can be

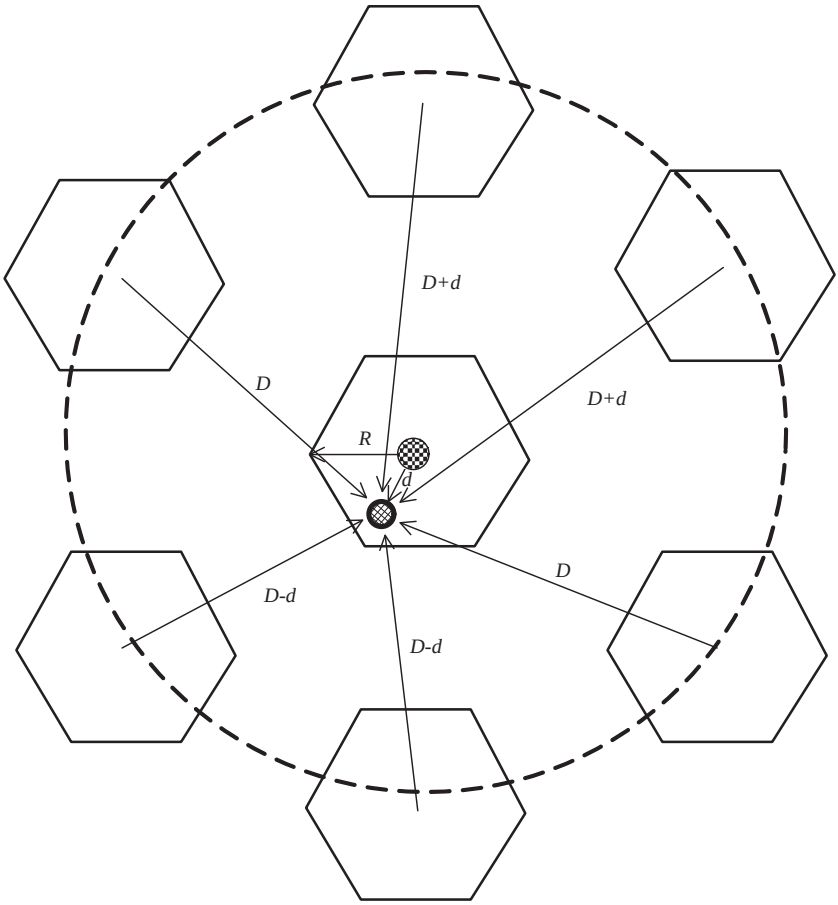

Fig. 9.1 Co-channel interference for the DL where the SS is at a distance d $(0 \leq d \leq R)$ from the centre of the cell (D is the reuse distance). The worst-case occurs when $d = R$

chosen at burst level, there is also the flexibility to in effect use different MCS by different users (even without sub-channelisation), as they may use consecutive bursts within a frame.

In snap-shot simulations, averaging the generated interference by just placing all SSs in the center of the cell is not the correct procedure due to the non-linear influence of pathloss at different distances [7]. The contributions to interference from SSs equally distributed all over the cell surface area needs to be taken into account [7]. However, in this paper, in our chosen analytical approach for Fixed WiMAX, we do not follow this approach. Instead we consider the worst-case interference scenario, where the UL interferer is located at the edge of the neighbouring cell whilst considering that the user at the central cell can move between the centre and the edge of the cell.

With omnidirectional antennas, the worst-case for interference geometry corresponds to the case where the SS in Fig. 9.1 is at the cell edge, hence $d = R$. The carrier-to-interference ratio in the DL is given by Eq. (8.11).

With tri-sectored cells (120° sectors), Eq. (8.11) becomes [8]:

$$C/I = \frac{1}{(r_{cc} + 0.7)^{-\gamma} + (r_{cc} - 0.22)^{-\gamma}}, \tag{9.1}$$

which is valid for both links; r_{cc} is given by (8.12). Note that in the omnidirectional case, the equation for the carrier-to-interference ratio in the UL results from the respective reuse geometry, where interferers are all at a distance *D-0.866R* from the central cell BS. This is given by:

$$C/I = \frac{(r_{cc} - 0.866)^{\gamma}}{6}. \tag{9.2}$$

These above equations only consider the first tier of co-channel interference: this assumption is generally only valid if a high value of the propagation exponent is used. If lower values for the propagation exponent are considered, interference to at least the second tier needs to also be considered [2]. To satisfy this, for example, for Eq. (8.11), terms proportional to $2\cdot(2r_{cc}+1)^{-\gamma}$, $2\cdot {r_{cc}}^{-\gamma}$ and $2\cdot(2r_{cc}-1)^{-\gamma}$ need to be added to the denominator.

The differences caused by the presence of sub-channelisation and sectorization can be interpreted by analysing the curves for *CNIR* as a function of the co-channel reuse factor, r_{cc}, with R as a parameter. To produce these curves, the power of the carrier is obtained by computing the power received by an SS at a distance R from the BS, while the computation of the interference depends on the UL and DL configuration, and also on the use of sectorization. This can be computed for a fixed R by making the same considerations for frequency reuse as in Eqs. (8.11), (9.1) and (9.2). For the sake of simplicity, the modified Friis equation is used with different values of the propagation exponent, γ, depending on the environment ($\gamma = 3$ is considered in many numerical examples, as it may be suggested from the experimental work in a suburban area from [4]). The noise power is computed by using the following equation:

$$N_{[dBW]} = -204 + 10 \cdot \log\left(b_{rf[Hz]}\right), \tag{9.3}$$

where b_{rf} is the channel radio frequency bandwidth. In the sub-channelisation case, b_{rf} should be divided by 16.

From these curves for the achievable *CNIR* as a function of r_{cc}, by considering the values of $CNIR_{min}$, it is straightforward to obtain the maximum supported physical throughput at the cell edge (distance R) in a simplified way, that is, by considering that users are uniformly distributed on the cell but not considering the mixture of services and applications and the exact details for the corresponding

"multiplexing" characteristics. For hexagonal-shaped cells, K = 1, 3, 4, and 7 correspond to reuse factors r_{cc} = 1.732, 3.000, 3.464, and 4.583. We have utilised these values.

The variation of *CNIR* with *rcc* without considering relays are presented in Chapter 8.

9.3 *CNIR* Versus Physical Throughput with Relays

9.3.1 Formulation

In this section the analysis of throughput is performed by considering the use of relays. In these topologies, a cell is composed by the central coverage area, served by the BS, and three 240° sector coverage areas, served by individual RSs (RS_1, RS_2 and RS_3), Fig. 9.2. While the BS backhaul is assured in the usual terms for mobile communications (e.g., cable or micro-wave radio link), RS backhauling is supported by using special specific sub-frames within the radio channel created for this purpose [9].

The central coverage area BS may have omnidirectional or tri-sectored antenna. In the latter case, if Frequency Division Duplexing (FDD) is considered, more channels are needed which, in turn, allows for making extra resources available to the RSs (as separate frequency channels are made available at itch sector).

While the BS backhaul is assured in the usual terms for mobile communications (e.g., cable or micro-wave radio link), RS backhauling is supported by using special specific sub-frames within the radio channel created for this purpose. Figure 9.3 shows the fixed WiMAX FDD mode frame structure assumed in this work.

The WiMAX frame is divided into DL and UL sub-frames which, in turn, include sub-sections with the following purpose, Fig. 9.3:

- BS to MS communications
- MS to BS communications

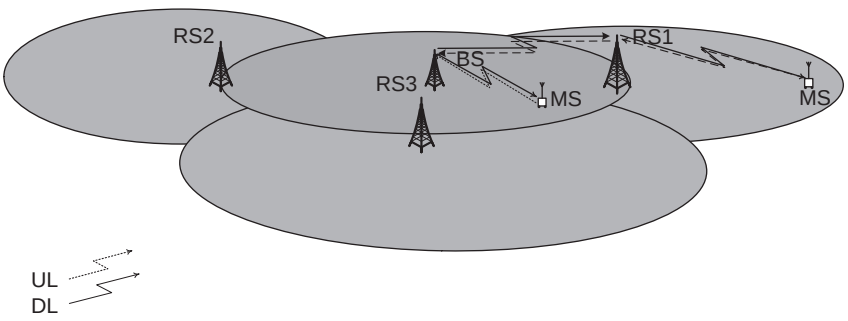

Fig. 9.2 BS, RS and respective "hexagonal" coverage areas

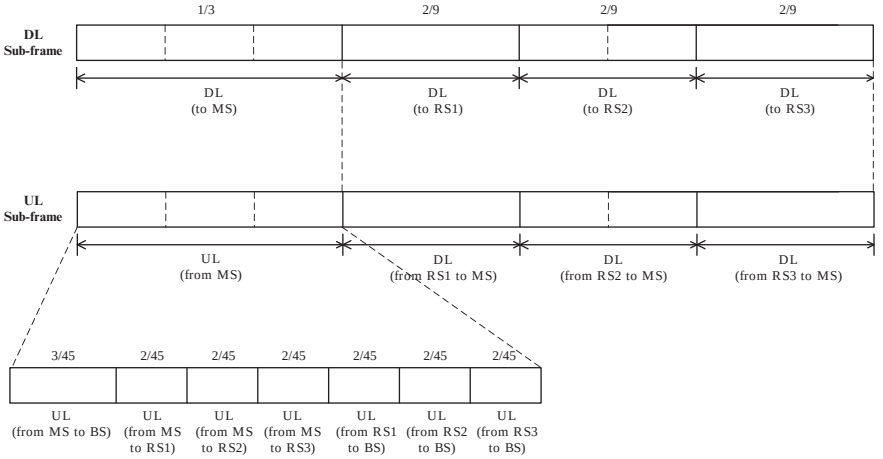

Fig. 9.3 Frame structure for UL and DL sub-frames with relays (omnidirectional BS)

- BS to RS communications
- RS to BS communications
- RS to MS communications
- MS to RS communications

It is worthwhile to note that the UL sub-frame supports DL communications from RS to MS. As we assume asymmetrical communications between the UL and DL with an asymmetry factor of 1/5 as shown in Fig. 9.3, the UL sub-frame may make these extra resources available for DL RS communications.

The advantage of using relays becomes from the fact that the co-channel interference now comes from cells at a longer distances because the real distance is given by:

$$D = 3\sqrt{k}R \tag{9.4}$$

The corresponding cell geometry is presented in Fig. 9.4. The cell is formed by a central coverage zone with hexagonal shape and three hexagonal outer coverage areas with 240° sectored antennas, as shown in Fig. 9.4, each occupying two thirds of the area relatively to the central coverage zone.

This different approach corresponds to consider three times the coverage area becomes [6, 7]:

$$A_{multihop} = 3.A_{singlehop} \tag{9.5}$$

Different cases are discussed for the DL and UL, for the communications from and to RS and BS.

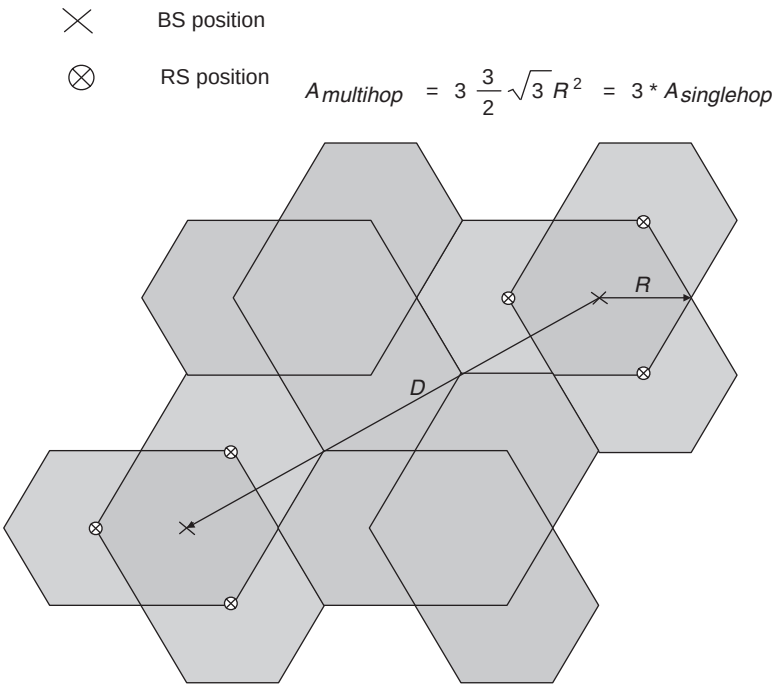

Fig. 9.4 Cell with RS at the edge of the central coverage area

9.3.2 Assumptions

A set of assumptions is considered in this research on frequency reuse for fixed WiMAX with relays with a frequency reuse pattern (or cluster size) $K = 3$.

For downlink (DL), the objective is to maximize the supported throughput. The optimization process is twofold [9]:

- The offered throughput from BS to RS needs to be maximized, that is, for a hexagonal coverage area with radius R the throughput $R_b(R)$ needs to be the highest possible.
- The offered throughput to SSs needs to be maximized. It is further be divided into two points:
- **Maximization of $R_{b\text{-}sup}$ at the SSs on the central coverage area –** By considering our assumptions for DL and UL frames (to cope with the Relay Station communications, Fig. 9.3) the DL throughput at the central coverage area is approximately 1/3 of the total one
- **Maximization $(R_{b\text{-}sup})_{RS}$ in SSs at the three relay coverage areas –** The maximum throughput at the RS coverage area is $R_{b-max}=min\{R_b(R), (R_{b-sup})_{RS}\}$ multiplied by 2/9, that is, $2/9 \cdot R_{b-max}$, where $R_b(R)$ is the maximum throughput at

the edge of the central cell, at a distance R from the BS, and $(R_{b\text{-}sup})_{RS}$ is the total throughput that may be supported at the RS coverage area if the Rs backhaul could support it (and considering the total frame duration)

Relay station antennas for the communication with the BS are considered to be directional (e.g., 120° sectored ones); so that they only receive/cause interference from/at two BSs at distance $D+R$, as it will be shown in the formulation.

From the communications at the relay, in our hypothesis for frames, it is only possible to achieve $2/9 \cdot R_{b-max}$ for the supported throughput at the whole RS coverage area. However, only if the BS to RS link supported throughput is enough the total throughput is guaranteed. In practice, the throughput at a distance d from the RS, $R_b(d)$ depends on the supported modulation and coding scheme (MCS), and is given by [9]:

$$R_b(d) = \frac{2}{9} R_b(R) \times AuxFactor(d) \tag{9.6}$$

where d is the distance to the RS and $R_b(R)$ is the maximum throughput at the edge of the central cell, at a distance R from the BS and $AuxFactor(d)$ is given in Table 9.1.

Let's assume as an example that the 16-QAM ½ MCS is supported in the central coverage area. Table 9.1 shows the values for $AuxFactor(d)$ if the MCS ID that may be guaranteed for the $CNIR(d)$ from the RS coverage area is 1, 2, 3, 4, 5, 6, 7 or 8. The 16-QAM ½ MCS is shown in bold in Table 9.1.

In practice, the rule for RS is the following: If the MCS supported at a distance d from the RS is higher or equal the one supported in the BS-to-RS link (16-QAM ½ in this example) the throughput for RS will be $2/9\ R_b(R)$; otherwise the throughput will be $2/9\ (R_{b\text{-}sup})_{RS}$.

For UL, the maximization of supported throughput, $R_{b\text{-}sup}$ is also twofold [9]:

- The supported throughput from RS to BS needs to be maximized. At the BS from RS it is only possible to achieve $2/45\ R_{b\text{-}sup}$
- The supported UL throughput needs to be maximized. It is further divided into two parts

Table 9.1 *AuxFactor* (*d*) for different values of the MCS ID for the communications to the SSs at RS coverage area

ID	MCS	CNIRmin (dB)	Physical thr. (Mbps)	AuxFactor(d)
1	BPSK ½	3.3	1.41	1.41/5.64
2	BPSK 3/4	5.5	2.12	2.12/5.64
3	QPSK ½	6.5	2.82	2.82/5.64
4	QPSK 3/4	8.9	4.23	4.23/5.64
5	16-QAM ½	12.2	5.64	1
6	16-QAM 3/4	15.0	8.47	1
7	64-QAM 2/3	19.8	11.29	1
8	64-QAM 3/4	21.0	12.27	1

- Maximization of the supported UL throughput at the RS (from MS) in the central coverage area (the maximum achievable throughput is 3/45 $R_{b\text{-}sup}$)
- Maximization of the offered throughput from SSs to RSs at the three RS coverage areas (the maximum is 2/45 $(R_{b\text{-}sup})_{SS}$)

Since relay station antennas are directional thus base station only receive interference from two BS at distance $D+R$. At the relays station it is only possible to achieve 2/45 $(R_{b-sup})_{SS}$, where $(R_{b-sup})_{SS}$ refers to the supported throughput from SS to RS. This traffic will only reach BS if the RS to BS radio link supports such value of the throughput.

9.3.3 DL Scenarios

For the DL there are three different cases that need to be individually analyzed:

1. **BS to SS**: BS to SS communication is the simple case Fig. 9.5 is discussed before the same formula for C/I is used as discussed in (8.23).
2. **BS to RS:** In the case of BS to RS communication one assumes that RSs are using directional antennas of 120° Fig. 9.6 and only receive interference from

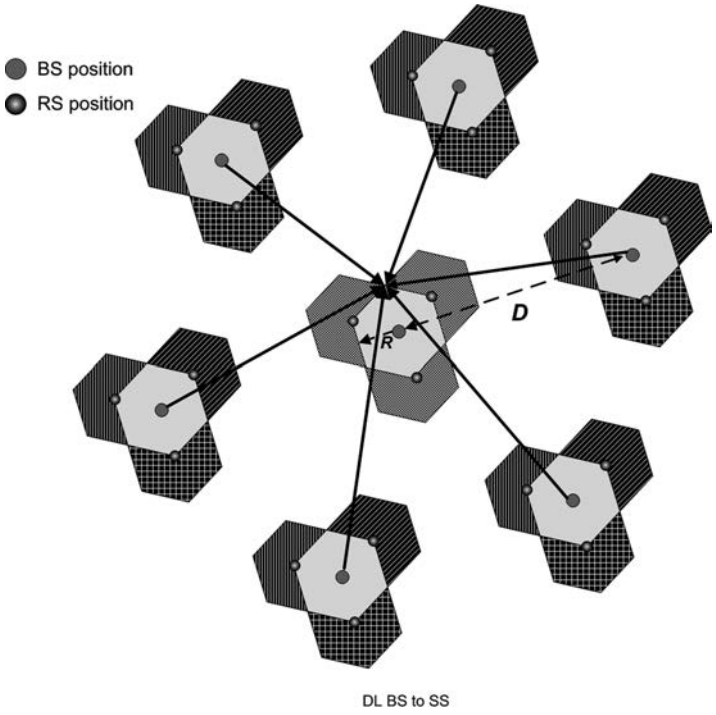

Fig. 9.5 DL scenario

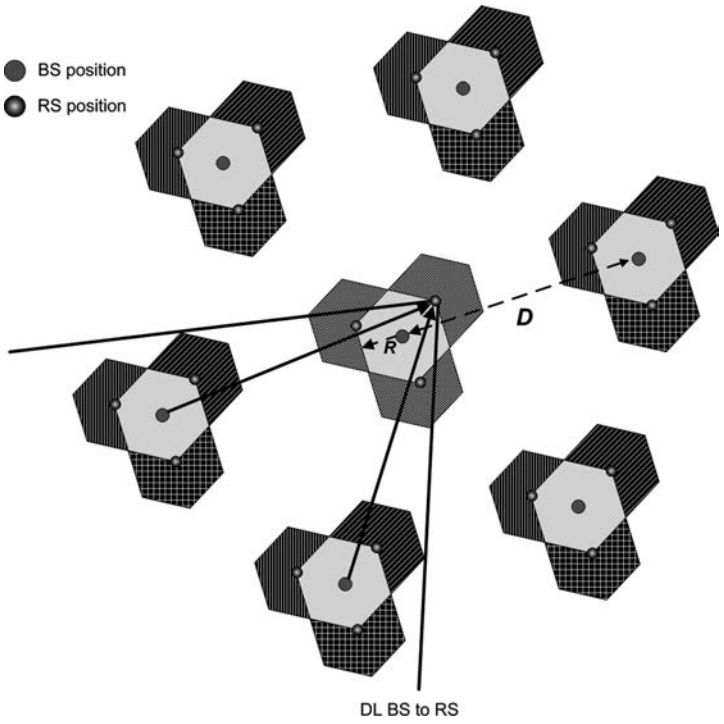

Fig. 9.6 DL scenario with 120° RS sectorial antennas and 240° sector RS coverage area

two BSs, Fig. 9.8. This ultimately effects and enhances the C/I by a significant amount as shown in the later discussion. Therefore $(D+\alpha R)^{-\gamma}/R^{-\gamma}=(r_{cc}+\alpha)^{-\gamma}$ has a coefficient 2 while $\alpha = 1$ and C/I is given by:

$$\frac{C}{I} = \left(\frac{1}{2(r_{cc}+1)^{-\gamma}}\right) \tag{9.7}$$

3. **RS to SS:** In the case of RS to SS, the SS receives interference from four neighbouring RSs, Fig. 9.7. The distances between cell centres, RS and SS shown in Fig. 9.5 measured by using Autocad 2008 in a worst case situation where RS is at the edge of the coverage area. On the basis of measured distances the coefficients of R, in$(D+\alpha R)^{-\gamma}$, are calculated as given below [9]:

$$D = 3R\sqrt{3} = 519.615\,\text{m} \tag{9.8}$$

$$R = 100\ \text{m} \tag{9.9}$$

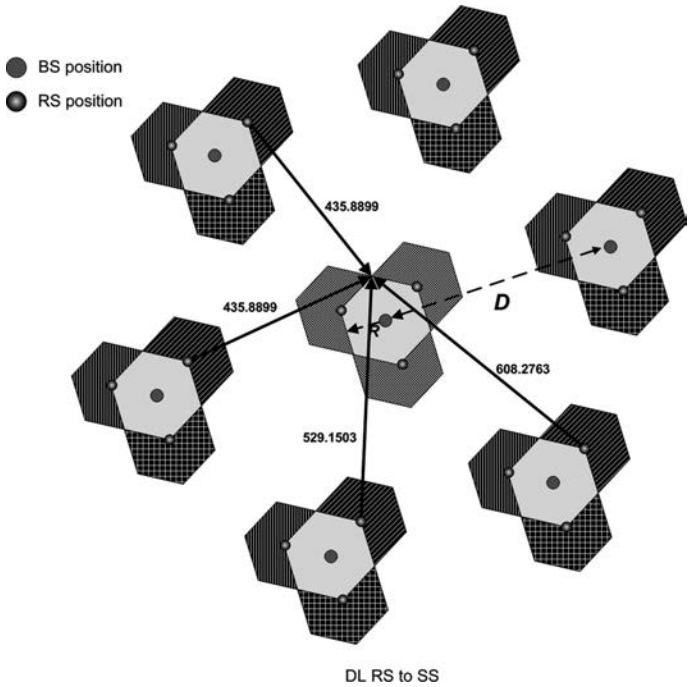

Fig. 9.7 Distances from the RS interferers to the SS

There are two RS at 435.8899 m from the envisaged SS:

$$\frac{435.89 - 519.62}{100} = -0.837 \tag{9.10}$$

There is one RS at 529.1503 m from the SS:

$$\frac{529.15 - 519.62}{100} = 0.0953 \tag{9.11}$$

and one at a distance 608.27 m:

$$\frac{608.28 - 519.62}{100} = 0.8866 \tag{9.12}$$

Hence, C/I is given by [9]:

$$\frac{C}{I} = \frac{R^{-\gamma}}{2(D - 0.8372R)^{-\gamma} + (D + 0.09535R)^{-\gamma} + (D + 0.8866R)^{-\gamma}} \tag{9.13}$$

9.3.4 UL Scenarios

For the UL there also are three different cases that need to be analyzed individually:

1. **From SS to BS:** In case of SS to BS there is interference from six surrounding SS. Thus carrier-to-interference ratio is given by

$$\frac{C}{I} = \frac{(r_{cc} - 0.866)^{\gamma}}{6} \tag{9.14}$$

2. **From RS to BS:** In this case we have assumed that RS antennas are 120° sectored one. Thus, the BS at the central cell only receives interference from two RS, at distance $D+R$, Figs. 9.8 and 9.9. The carrier-to-interference ratio is given by

$$\frac{C}{I} = \frac{(r_{cc} + 1)^{\gamma}}{2} \tag{9.15}$$

3. **From SS to RS:** In this case RS receives interference from four SSs in neighbouring cells. By using the same procedure to measure the distances

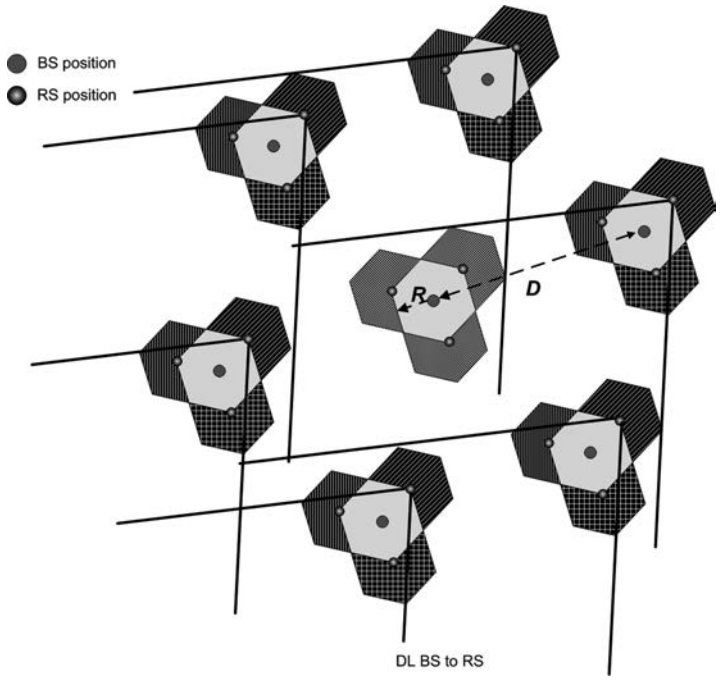

Fig. 9.8 The decrease of the co-channel interference by using directional antennas at RS

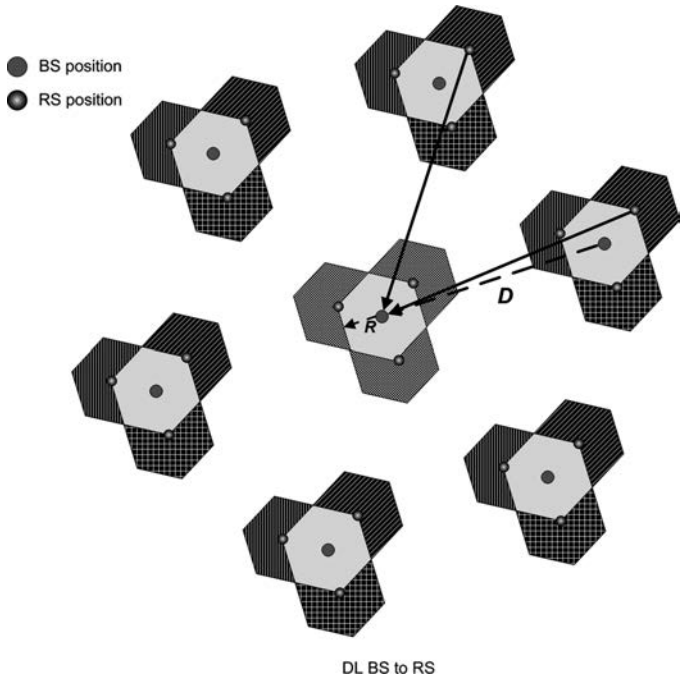

Fig. 9.9 Distances from RS to BS in the UL

between cell centres, RS and SS, the following values were obtained for the coefficients α of R: -0.8761, -0.82776, -0.80762. As a consequence, C/I is given by:

$$\frac{C}{I} = \frac{R^{-\gamma}}{2(D-0.8761R)^{-\gamma} + (D-0.082776R)^{-\gamma} + (D-0.80762R)^{-\gamma}} \tag{9.16}$$

9.4 Supported Physical Throughput

9.4.1 Implicit Function Formulation

To guarantee Fixed WiMAX coverage with no coverage gaps near cell edges, the *CNIR* must be higher than 3.3 dB throughout the cell. This value corresponds to the minimum *CNIR* in order to use the BPSK ½ MCS (see Table 9.1).

The assessment of the supported cell/sector physical throughput (per transceiver), R_b, as a function of the distance, d, produces a staircase-shaped curve

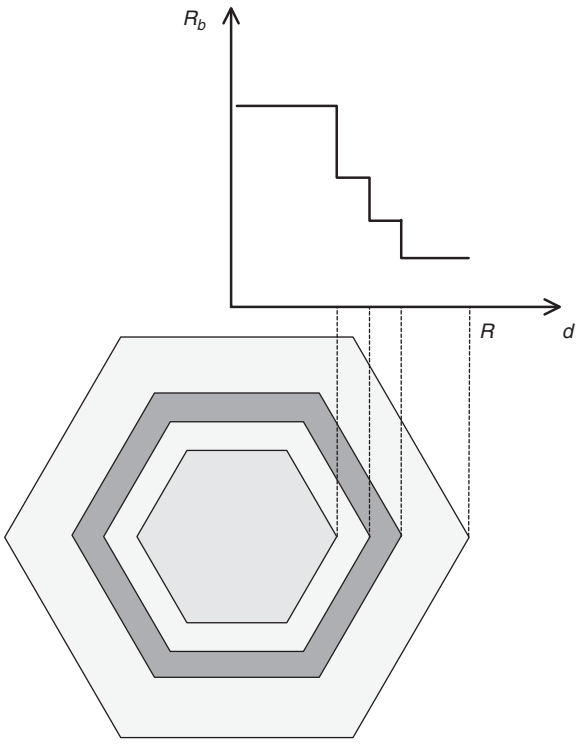

Fig. 9.10 Areas of the coverage rings where a given value of physical throughput is supported

indicating that higher maximum achievable throughputs are supported near the centre of the cell (see Fig. 9.10). As throughput is not constant over the whole coverage area for cellular planning proposes (where R is the cell radius), the supported throughput is obtained by computing the average supported throughput in the cell. As stated previously, in contrast to [6, 7], worst-case scenarios for interference geometry are considered here.

There are J different coverage rings in each coverage zone, each supporting a different MCS (for instance, $J = 4$ in Fig. 9.10). The distances that correspond to the steps between consecutive MCS are represented by d_j, $j = 1, 2, \ldots, J$. Here we denote the order of the MCS as MCS_j. The number of different coverage rings is given by:

$$J = MCS_{1^{st}} - MCS_{last} + 1, \tag{9.17}$$

where $MCS_{1^{st}}$ and MCS_{last} represent the MCS for the first and last coverage rings, respectively.

If only one frequency channel is considered per cell, the supported throughput is obtained as [8, 10]:

$$R_{b-\sup} = \frac{\iint_{O} R_b(d,R,K)dxdy}{\frac{3\sqrt{3}}{2}\cdot R^2} = \frac{\sum_{j=1}^{J}\left(\frac{3\sqrt{3}}{2}\cdot\left(d_j^2 - d_{j-1}^2\right)\cdot\left(R_b\right)_{MCS_{1st}+1-j}\right)}{\frac{3\sqrt{3}}{2}\cdot R^2}, \quad (9.18)$$

where the 2D integral is performed over the hexagonal shape of the cell. It is computed by weighting the supported physical throughput in each concentric coverage ring by the size of the ring where that value is supported. The contribution of each of the transmission modes is thus considered.

$MCS_1{}^{st}$, $MCS_2{}^{nd}$, …, $MCS_J{}^{th}$ can be obtained in the following way

$$MCS_j\left(CNIR_{[dB]}\right) = \begin{cases} 0, CNIR<3.3 \\ 1, 3.3\leqslant CNIR<5.5 \\ 2, 5.5<CNIR<6.5 \\ 3, 6.5<CNIR<8.9 \\ 4, 8.9<CNIR<12.2 \\ 5, 12.2<CNIR<15.0 \\ 6, 15.0<CNIR<19.8 \\ 7, 19.8<CNIR<21.0 \\ 8, CNIR>21.0 \end{cases}, \quad (9.19)$$

where j represents the coverage ring, $CNIR_{[dB]} = 10\cdot\log(cnir)$, and $MCS_k = 0$ means that there is not enough coverage in that part of the cell (or coverage ring); in this case, the system will not be viable. Besides, if $l = MCS_j$, one can represent the physical throughput corresponding to each MCS, l = 0,1, …, 8, as

$$\left(R_b\right)_l = \begin{cases} 0, l=0 \\ 1.41, l=1 \\ 2.12, l=2 \\ 2.82, l=3 \\ 4.23, l=4 \\ 5.64, l=5 \\ 8.47, l=6 \\ 11.23, l=7 \\ 12.27, l=8 \end{cases}. \quad (9.20)$$

$CNIR(R_b)$ is not a bijective function. Therefore, the value of $CNIR$ that corresponds to a given R_b is the minimum value of $CNIR$, that is, $CNIR_{min}$, that supports a given throughput R_b. Hence $d_0 = 0$, and

$$d_j = cnir^{-1}\left(\min\left(CNIR\left(\left(R_b\right)_{MCS_{1st}+1-j}\right)\right)\right), j = 1,\ldots,J. \quad (9.21)$$

Figure 9.11 presents the correspondence between the $CNIR$ vs. propagation distance curve and the stepwise function that represents the $CNIR_{min}$ threshold for each MCS versus R_b. This Figure illustrates how the mapping between $CNIR$ and

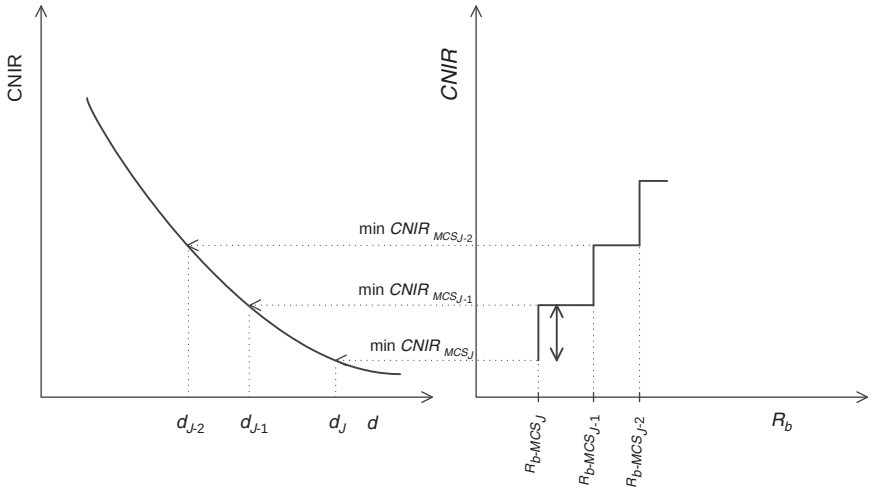

Fig. 9.11 Correspondence between the physical throughput for rings J, $J-1$, $J-2$, ..., and the minimum *CNIRs* of consecutive MCS that map to step distances d_J, d_{J-1}, d_{J-2}, ...

supported physical throughput relates to step distances between consecutive MCS d_J, d_{J-1}, d_{J-2}, ...

This Figure illustrates how the mapping between *CNIR* and supported physical throughput relates to step distances between consecutive MCS d_J, d_{J-1}, d_{J-2}, ...

In the context of the experimental work performed within our research group, results have fitted the modified Friis equation to some ranges of coverage distances in Fixed WiMAX [4]. According to the modified Friis equation, the received power is given by

$$p_r(d) = \frac{p_t \cdot g_t \cdot g_r \cdot \lambda^2}{(4\pi)^2 d^\gamma}. \tag{9.22}$$

where $0 \leq d \leq R$, λ is the wavelength, P_t, G_t and G_r (the latter ones are in dB), and γ is the propagation exponent.

9.4.2 Without Relays

In the DL, for a given R, the reuse distance is given by $D = r_{cc} \cdot R$, and the interference at a distance d from the BS is computed by the following approximate equations

$$i(d,D,R) = \frac{p_t g_t g_r \lambda^2}{(4\pi)^2} \left(\frac{2}{(D-d)^\gamma} + \frac{2}{D^\gamma} + \frac{2}{(D+d)^\gamma} \right), \tag{9.23}$$

$$i(d,D,R) = \frac{p_t g_t g_r \lambda^2}{(4\pi)^2}\left(\frac{1}{(D-0.7\cdot d)^{\gamma}} + \frac{1}{(D-0.22d)^{\gamma}}\right). \quad (9.24)$$

Equation (9.23) is applied in the omnidirectional BS antenna case while Eq. (9.24) is applied in the tri-sectored case. Under sectorization, only two interference sources need to be considered. Although these formulas are both valid for the DL (9.24) is also valid for the UL. For the omnidirectional case on the UL, Eq. (9.2) for interference can still be applied as it does not depend on d, as the distances from the SS interferes to the cell BS are *D-R*. Note that, as for Eqs. (8.11), (9.1) and (9.2), the second tier of interference would also need to be considered if lower values of the propagation exponent were used.

We are aware that in this paper we do not consider per sub-channel equivalent *SINR* (or *CNIR*) computations when sub-channelisation is used. These computations could be performed accounting either for exponential effective *SINR* mapping (EESM [11–14]), effective code rate map (ECRM), or mean instantaneous capacity (MIC [6]). The consideration of these compression techniques may be needed in the presence of selective fading to adapt the curves to actual *CNIR*s in the UL.

In the following, five different cases are addressed:

- The DL in the absence of sub-channelisation and sectorization (which we denote as the "DL – omnid". case)
- The UL in the absence of sub-channelisation and sectorization (the "UL– omnid". case)
- The UL in the presence of sub-channelisation and absence of sectorization (the "UL – sub-channel". case)
- The UL and DL in the absence of sub-channelisation and the presence of sectorization (the "UL & DL – sector". case) and
- The UL in the presence of sub-channelisation and sectorization (the "UL – subch. & sector". case).

Figure 9.12 presents the curves for $R_b(d)$ for $K = 4$ with a coverage distance $R =$ 2,500 m. Without using sub-channelisation or sectorization, the DL performance is clearly better than the UL one. However, when sectorization is considered, higher physical throughputs are achievable. Besides, the better results are obtained when both sub-channelisation and sectorization are used. In this case, the highest physical throughput reaches 12.27 Mb/s, which is achieved for distances up to $d \approx 1{,}500$ m.

As an example, Fig. 9.13 presents a comparison of the results for the cell physical throughput for different reuse patterns $K = 1$, 3, 4 and 7, for "UL – subch. & sector". and $R = 2{,}500$ m.

If one carefully analyses the difference in the areas below the curves in these Figures, the following conclusions can be extracted:

- Although the physical throughput clearly increases with the use of sectorization only with the simultaneous use of sectorization and sub-channelisation in the UL the highest order MCSs are possible near the cell edge.

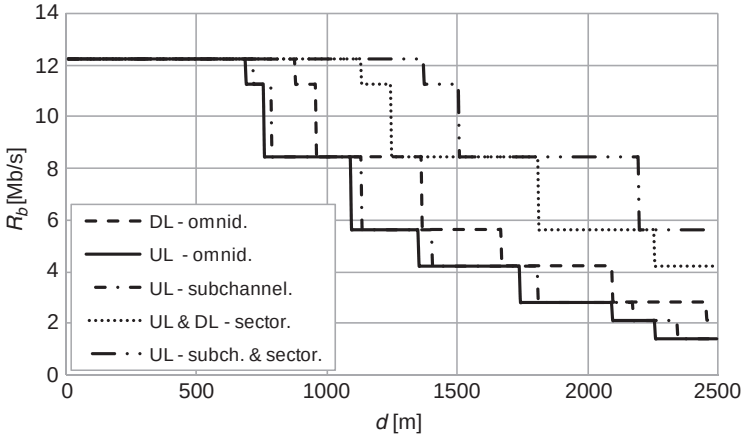

Fig. 9.12 Example of the variation of the physical throughput as a function of d for R = 2,500 m and K = 4

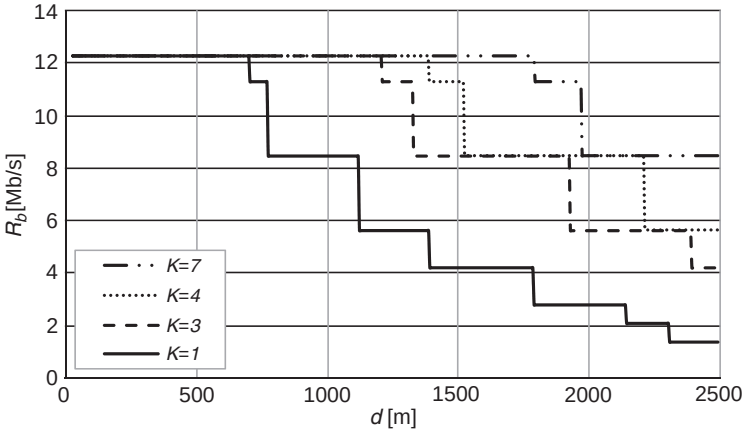

Fig. 9.13 Variation of the physical throughput in the "UL – subch. & sector." case versus d, for R = 2,500 m

- With no improvement technique the DL performs better than the UL.
- A value for the reuse pattern K = 7 only presents a slight advantage relatively to the consideration of K = 4 or 3, whose behaviour is very similar; this is mainly true in the "DL" and "UL & DL – sector". Cases, whose curves are not presented here. It should be noted here that K = 1 is not supported without the use of sectorization.

By applying Eq. (9.18) to the results for the cell physical throughput (as the ones from Figs. 9.12–9.13), one obtains the curves for the supported throughput as a

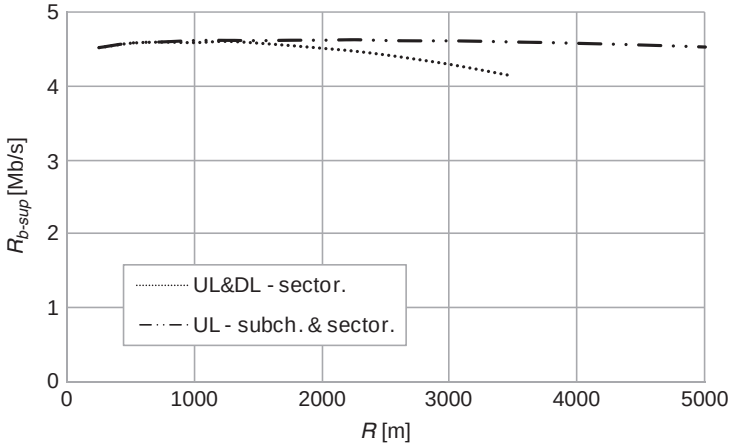

Fig. 9.14 Supported sector physical throughput versus R for $K = 1$

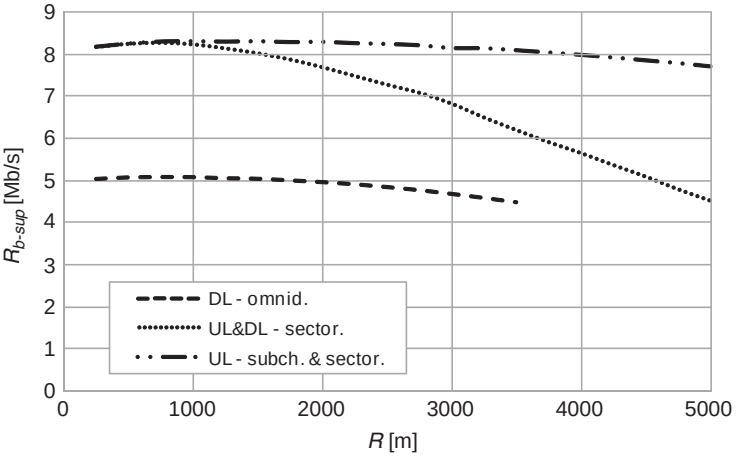

Fig. 9.15 Supported cell/sector physical throughput versus R for $K = 3$

function of R for $K = 1, 3, 4$ and 7 presented in Figs. 9.14 through 9.17, respectively. Some of the curves with no sub-channelisation are either impossible to obtain at all or after a given R, for example, for $K = 1$, 3 or 4. This is because the physical throughput on the outer coverage ring of the cell reaches 0 Mb/s and full cell coverage may not be guaranteed. The supported throughput results for $K = 4$ are slightly worse than the ones for $K = 7$ but they are still acceptable (where there is the advantage under $K = 4$ of using only 4/7 = 57% of the spectrum bandwidth).

For $K = 3$, although the degradation compared to $K = 7$ seems high compared with $K = 4$, only 3/4 = 75% of the bandwidth is used. This reduction in spectrum bandwidth is, however, not as much as between $K = 7$ and $K = 4$. Using $K = 1$ is

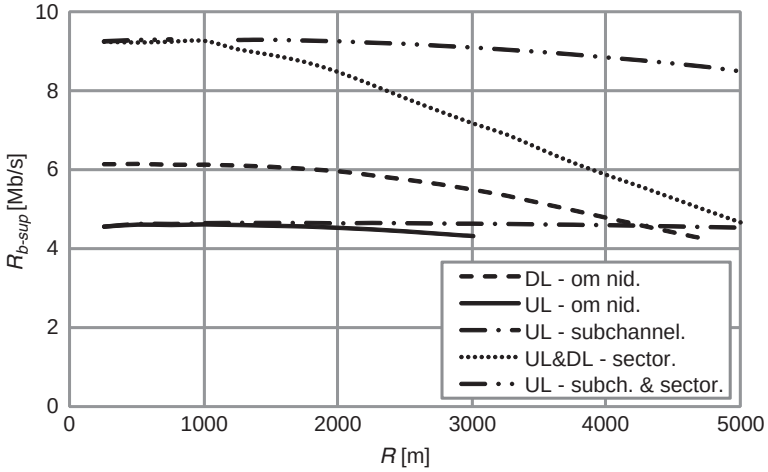

Fig. 9.16 Supported cell/sector physical throughput versus R for $K = 4$

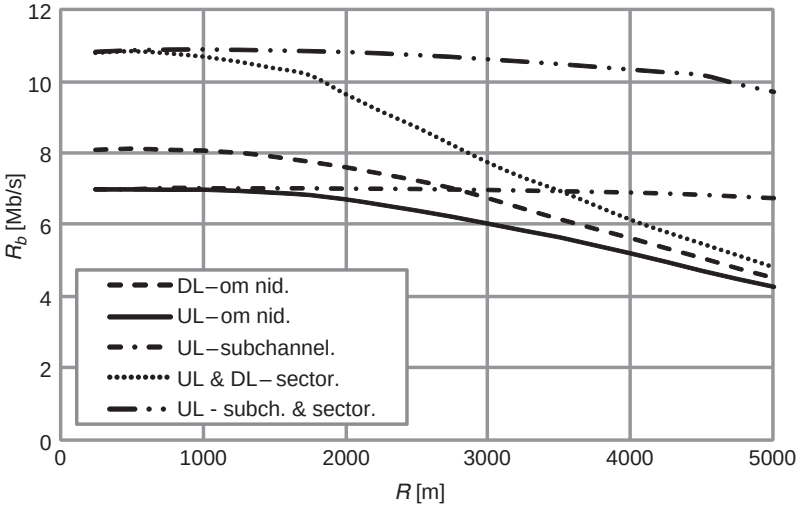

Fig. 9.17 Supported cell/sector physical throughput versus R for $K = 7$

advantageous because only a small portion of spectrum is needed. If tri-sectorization is used, as sub-channelisation is not supported in the DL, a fractional use of the WiMAX channels is not possible and three different channels are needed, one for each sector.

In this case, the total supported throughput is three times the sector average throughput. With 3.5 MHz channels, only 10.5 MHz are needed for each link direction.

Table 9.2 Average supported throughput for low coverage distances with different Ks with simple assumptions

$\overline{R_{b-\sup}}$	DL – omnid.	UL – omnid.	UL &DL – sector.	UL – sector. & subch.
$K = 1$	–	–	4.515	4.591
$K = 3$	5.051	–	8.160	8.241
$K = 4$	6.100	4.623	9.149	9.255
$K = 7$	8.024	6.985	10.689	10.813

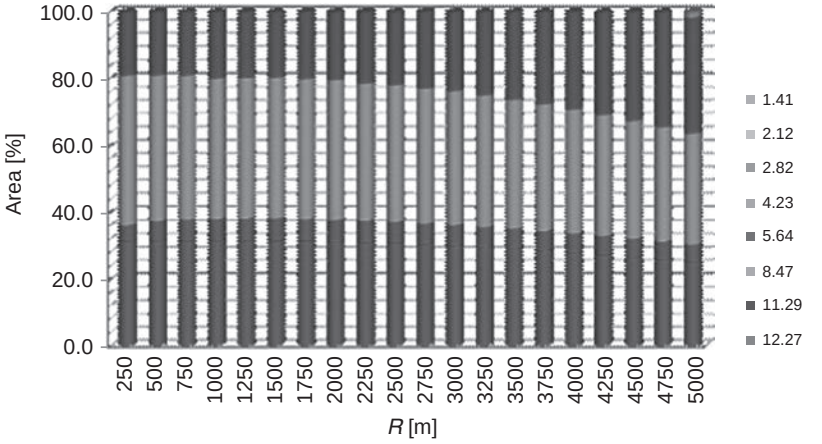

Fig. 9.18 Area covered by each MCS versus R for $K = 4$, in the "UL – subch. & sector" case

It is however worthwhile to compare results for the supported throughput among different values of K by assuming, for the sake of simplicity, that only one single channel could be used (even with tri-sectorization). For short coverage distances, that is, up to 1,500–2,500 m, depending on the cases (the highest Rs occur with sub-channelisation), the average values of achievable supported throughput are presented in Table 9.2.

When K decreases, if sectorization is not used the reduction in physical throughput is higher; that is, high values of throughput are only achievable through the use of sectorization. Moreover, for this range of coverage distances, the values of supported throughput are only ∼1–2% lower without sub-channelisation compared with the case where both sub-channelisation and sectorization are used.

The comparison between the "UL – sector. & subch". and "DL" cases shows a reduction in the supported throughput for the DL case of 38.7, 34.1, and 25.8%, for $K = 3$, 4, and 7, respectively (note that for $K = 1$, it is not possible to support users in the DL without sectorization). While with omnidirectional antennas there is a clear asymmetry between UL and DL traffic (see Figs. 9.16 and 9.17) it is evident that the UL and DL can be balanced through the use of sectorization.

These curves can be better interpreted by analysing the variation with R of the cell area, in percentage, corresponding to each supported data rate, that is, for each MCS (according to Table 9.1). Figure 9.18 presents the corresponding curves for

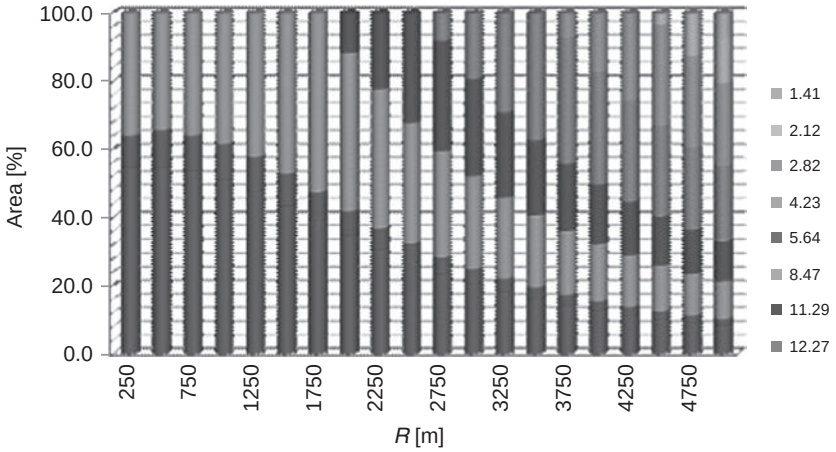

Fig. 9.19 Area covered by each MCS versus R for $K = 7$, in the "UL & DL – sector" case

$K = 4$ in the "UL – subch. & sector" case. From this, it can be observed that the highest values of the throughput are supported in the presence of sub-channelisation plus sectorisation, and correspond to the exclusive operation with the four highest order MCS for coverage distances of up to 4,750 m.

Figure 9.19 presents the variation of the coverage area, in percentage, against R, for each MCS, but this time for the case $K = 7$ and "UL – subch. & sector", which is presented as an example.

By comparing these results with the ones for $K = 4$ one concludes that, for $K = 7$, the three highest order MCS are only supported up to $R = 1{,}750$ m, whereas, for $K = 4$, four different MCS are needed. However, for $K = 7$ and coverage distances higher than 2,500 m, the trend of enabling larger coverage distances while solely using the highest order MCS is not maintained anymore.

9.4.3 DL with Relays

The Fig. 9.20 shows the throughputs of the different scenarios of DL.

1. **From BS to MS:** Throughput from BS to MS is sufficiently high and it gradually decreases with the increase of the cell coverage distance R. In our assumptions, the frame structure is assigned 1/3 for DL. So, the DL throughput is obtained by the multiplying this factor 1/3 by the total obtained one. If we want to compare this value with the throughput in the RS coverage area, as they only have the coverage area, a normalized should be needed that is obtained by multiplying the throughput by this factor 2/3.
2. **From BS to RS:** The throughput from RS to BS remains high at constant level until 4 km and then suddenly decreases after 4 km. This throughput is obtained

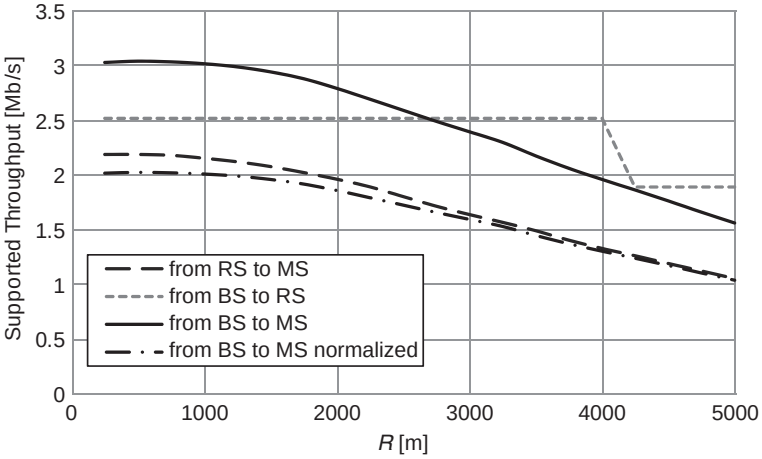

Fig. 9.20 Results for the supported throughput as function of R in the DL with relays ($K = 3$, omnidirectional BS)

by using directional antennas at RS which greatly decreases the co-channel interference, Fig. 9.5. Only two RS receive interference from the central cell BS.

$$i(d) = \frac{P_t G_t G_r \lambda^2}{(4\pi)^2} (D + d)^{-\gamma} \tag{9.25}$$

The receiver antenna gain G_r value was set to 28 dBi to obtain this throughput.

3. **From RS to SS**: The throughput for RS to SS is almost of same value as BS to SS. In our assumptions the frame structure is assigned 2/9 in case of RS to SS for DL. So, this is obtained by the multiplying this factor to the total obtained throughput.

9.4.4 UL with Relays and K = 3

Figure 9.21 show the results for throughput for different UL scenarios.

1. **From SS to BS:** Throughput for SS to BS resembles the previous scenarios of DL. Throughput decreases with the increasing cell coverage area R. In our assumptions, for SS to BS, the frame structure is assigned 3/45 for UL. So, the UL throughput is obtained by multiplying this factor 3/45 the total obtained one. If we want to compare this value with the throughput in the RS coverage area, as they only have the coverage area, a normalized should be needed that is obtained by multiplying the throughput by this factor 2/3.

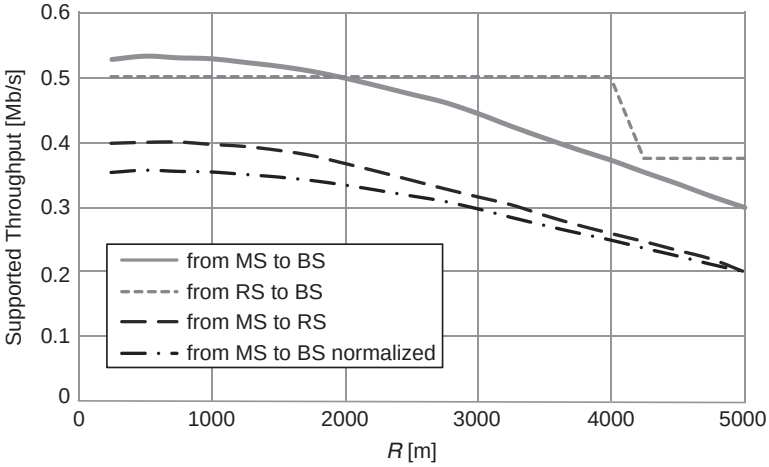

Fig. 9.21 Results for the supported throughput as function of R in the UL in the absence of sub-channelisation ($K = 3$)

2. **From RS to BS:** The throughput from RS to BS remains high at constant level until 4 km and then suddenly decreases after 4 km. This throughput is obtained by the use of directional antennas at RS which greatly decreases the co-channel interference, Fig. 9.8. The receiver antenna gain G_r value is set to 28 dBi to obtain this throughput.
3. **From SS to RS:** Throughput for SS to RS is almost of same value as SS to BS. In our assumptions, for SS to RS, the frame structure is assigned 2/45 for UL. So, this is obtained by the multiplying this factor to the total obtained throughput.

9.4.5 Use of Sub-Channelisation

In the case of IEEE 802.16-2004 standard does not support the sub-channelisation for DL. However, it may be supported in the UL. Therefore, to obtain the sufficient level of throughput for UL the sub-channelisation is used. Throughput analysis for the UL scenario from the Fig. 9.22 is performed with sub-channelisation. The main change is the fact that the throughput from RS to BS now remains constant when the cell coverage area varies. However, there are no remarkable differences in the other curves.

The throughput analysis from Fig. 9.11 for UL scenario is presented with sub-channelisation. In the case of RS to BS throughput the main change is the fact that the throughput from RS to BS now remains constant when the cell coverage area increases. So, there is constant level of throughput at all distances of cell coverage area R. However, one can see from the results that there is no remarkable difference in the other curves.

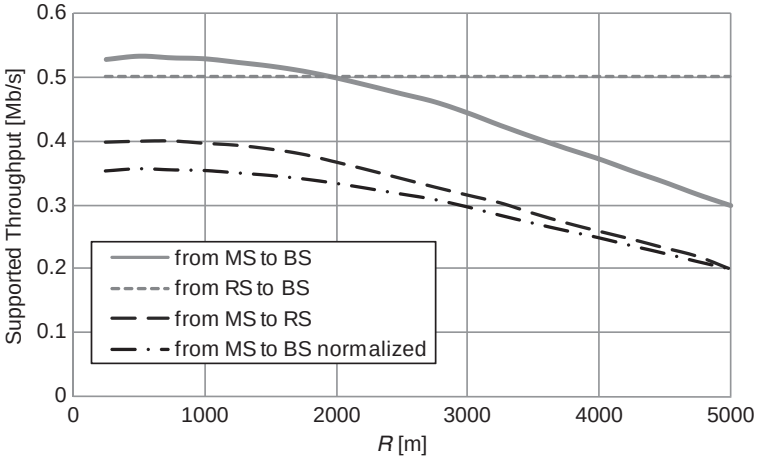

Fig. 9.22 Results for the supported throughput as function of R in the UL with sub-channelisation ($K = 3$)

9.5 Throughput with Sectorization, Relays and $K = 1$

The analysis with $K = 1$ was tried with omnidirectional cells but the communication from MS to BS was impossible. As the topologies with RSs are more favourable, it is worthwhile to consider tri-sectored antennas at the BS of the central coverage area. We used Eq. (8.23) to compute the carrier-to-interference ratio from/to the BS at the central cell (for DL and UL, respectively) but now with $D = 3\sqrt{k}R$.

The formulation for the communications between RSs and MSs is the same, as well as the one for the communications between RSs and BSs. By considering tri-sectored antennas we need to have one different channel (i.e., frequency carrier) for each sector. This way, more resources are made available to the RSs, and we can consider the assumptions from Fig. 9.23 for the DL and UL sub-frames. The asymmetry factor between the UL and DL is 3/7 in this case.

Figures 9.24 and 9.25 show the results for the supported throughput for the DL and UL, respectively. Although the supported throughput per channel may be lower (e.g., 8.25 Mb/s at 750 m against 9.79 Mb/s in the omnidirectional case), the supported throughput from BS to SS (with $K = 1$, tri-sectorization) is clearly higher than the one for "$K = 3$, omnidirectional BS" (e.g., a normalized throughput of 3.30 Mb/s in tri-sectored case at 750 m against 2.02 Mb/s in the omnidirectional case). This is owing to the more favourable frame format (the asymmetry factor is 3/7 against 1/5 in the omnidirectional case).

Nevertheless, with tri-sectorization and $K = 1$ it is a worth noting that the BS to SS communication is not the most limitative one anymore. In fact, the RS to SS link shows now the lowest throughput (e.g., 2.17 Mb/s for $R = 750$ m). These values are still slightly larger than the achievable ones in the omnidirectional central coverage area case with $K = 3$. Besides, it is worthwhile to note that, as there is one channel

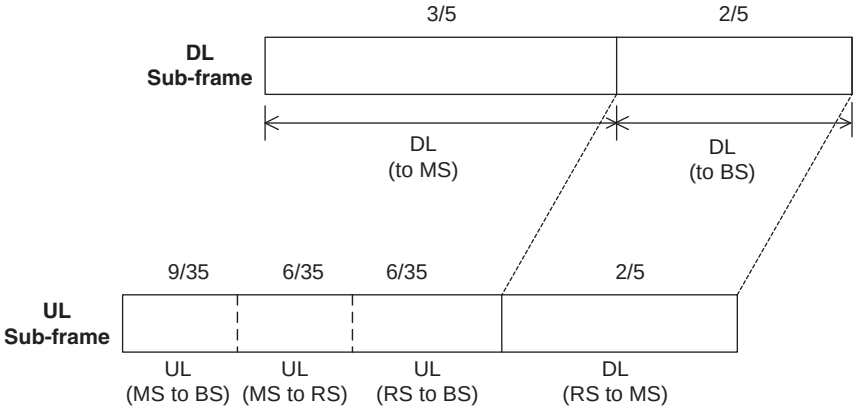

Fig. 9.23 Frame structure for UL and DL sub-frames with relays (tri-sectored BS)

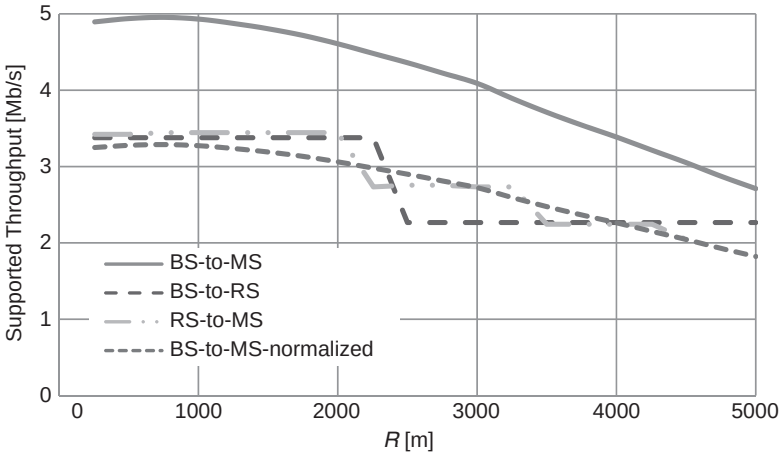

Fig. 9.24 Results for the supported throughput as function of R in the DL with relays (K = 1, tri-sectored BS)

assigned to each sector the total cell throughput (to be fed into the cost/revenue optimization procedure) is achieved by multiplying this sector throughput by three.

In the future, we also may analyse the presence of sub-channelization in the UL with K = 1, and its impact for the longest coverage distances. The case with tri-sectorized BS antenna and K = 3 is analyzed in [9].

9.6 Conclusions

In this work, a model to compute the supported physical throughput as a function of the achievable *CNIR* has been proposed for Fixed WiMAX. Frequency reuse topologies have been explored for 2D geometries that are commonly used in rural

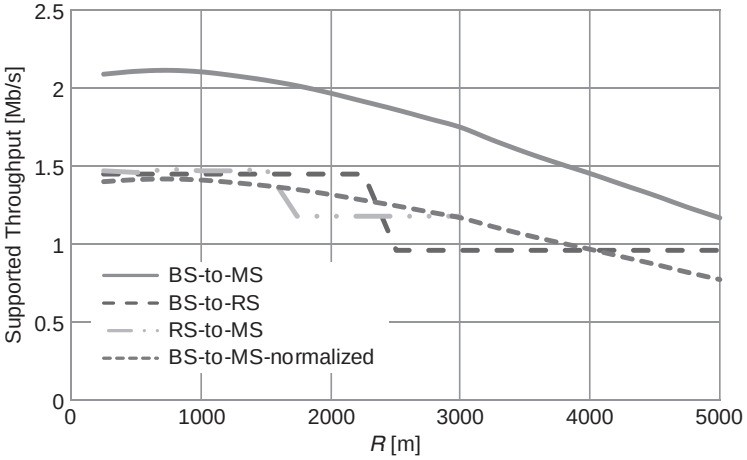

Fig. 9.25 Results for the supported throughput as function of R in the UL with relays (K = 1, tri-sectored BS)

and suburban environments, and the basic limits for system capacity and cost/revenue optimisation have been obtained by considering simple assumptions. It is assumed that line of sight propagation to the bases station is achieved in a high percentage of the cell, reducing the impact of selective fading, through allowing dimensioning to be done by GIS cellular planning tools.

For a given coverage area, throughput is a stepwise function that decreases as the distance to the base station increases. Its value depends on the supported MCS for each coverage ring. In this chapter, the supported throughput has been computed by weighting the available throughput at each coverage ring with the area (or size) of the ring. Throughput typically decreases as the cell radius increases, although through the use of sub-channelisation it is possible to keep its value steady at least up to a cell radius of 5,000 m. With the use of sectorization, the supported throughput is higher, corresponding to the use of the highest order MCSs. However, as sectorised equipment is more expensive and there is a need for three times more bandwidth, costs are also higher.

In this Chapter formulations were also proposed to account for the interference in cellular coverage and reuse geometries without and with the use of relay. In our proposal for relays, the FDD mode is considered and the frames need to guarantee resources for BS-to-MS communications but also for BS-to-RS and RS-to-MS communications. These requirements leads to a 1/5 asymmetry factor between the UL and DL in the omnidirectional BS case and to a 3/7 asymmetry factor in the case of tri-sectored BSs.

Although the reuse distance is augmented by a factor of $\sqrt{3}$, it was first shown that the use of relays corresponds to lower values of the supported throughput for $K = 3$. The presence of sub-channelisation only improves the results for the highest values of R.

The consideration of tri-sectored BS antennas with $K = 1$ (whilst keeping the number of required channels – equal to 3) did not enable to obtain values of the throughput comparable to the ones without using relays, although frame format is more favourable.

Relays can be cheaper than BS with full functionalities. As the use of relays may lead to lower costs it is worthwhile to analyse the impact of using them on costs and revenues.

References

1. G. Bauer, R. Bose, R. Jakoby, Three-dimensional interference investigations for LMDS networks using an urban database. IEEE Trans. Antennas Propag. **53**(8), 2464–2470 (Aug 2005)
2. F.J. Velez, L.M. Correia, J.M. Brázio, Frequency reuse and system capacity in Mobile Broadband Systems: comparison between the 40 and 60 GHz bands. Wireless Pers. Commun. **19**(1), 1–24 (Aug 2001)
3. T.S. Rappaport, *Wireless Communications: Principles and Practice* (Prentice Hall, Upper Saddle River, NJ, 2002)
4. P. Sebastião, F. Velez, R. Costa, D. Robalo, A. Rodrigues, Planning and deployment of WiMAX networks. WIRE – Wireless Pers. Commun. (Aug 2009). doi: 10.1007/s11277-009-9803-3
5. Hui Liu, Guoqing Li, *OFDM-based Broadband Wireless Networks – Design and Optimization* (Wiley, Hoboken, NJ, 2005)
6. J.G. Andrews, A. Ghosh, R. Muhamed, *Fundamentals of WiMAX – Understanding Broadband Wireless Networking* (Prentice Hall, Upper Saddle River, NJ, 2007)
7. C. Hoymann, S. Goebbels, Dimensioning cellular WiMAX part I: singlehop networks, in *Proceedings of EW'2007 – European Wireless 2007* (Paris, France, Apr 2007)
8. F.J. Velez, V. Carvalho, D. Santos, R.P. Marcos, R. Costa, P. Sebastião, A. Rodrigues, Aspects of cellular planning for emergency and safety services in mobile WiMax networks, in *Proceedings of ISWPC' 2006 – 1st International Symposium on Wireless Pervasive Computing 2006*, Phuket, Thailand, Jan 2006
9. F.J. Velez, M.K. Nazir, A.H. Aghvami, O. Holland, D. Robalo, Cost/revenue Trade-off in the optimization of Fixed WiMAX Deployment with Relays, submitted to IEEE Transactions on Vehicular Technology (Dec 2009)
10. F.J. Velez, A.H. Aghvami, O. Holland, Basic Limits for Fixed WiMAX Optimization Based in Economic Aspects, accepted for publication in IET Communications – Special Issue on WiMAX Integrated Communications (Mar 2009)
11. R. Jain, Chakchai So-In, A.-K. Al Tamimi, System-level modeling of IEEE 802.16e mobile WiMAX networks: key issues. IEEE Wireless Commun. **15**(5) (Oct 2008)
12. Sergey N. Moiseev, Stanislav A. Filin, and Mikhail S. Kondakov, Analysis of the Statistical Properties of the Interference in the IEEE 802.16 OFDMA Network, IEEE Wireless Communications and Networking Conference (WCNC 2006), vol. 4, pp. 1830–1835, Apr 2006
13. M.S. Kondakov, A.V. Garmonov, Do Hyon Yim, Jaeho Lee, Sunny Chang, Yun Sang Park, Analysis of the statistical properties of the interference in the IEEE 802.16 OFDMA Network, in *Proceedings of WCNC 2006 – IEEE Wireless Communications and Networking Conference*, Las Vegas, Nevada, USA, Apr 2006
14. 3GPP, *3rd Generation Partnership Project; Technical Specification Group Radio Access Network; Feasibility Study for OFDM for UTRAN Enhancement* (Release 6), 3GPP TR 25.892 V2.0.0, 2004-06